Archives of Materials Science and Engineering

Volume 41
Issue 1
January 2010
Pages 28-36

International Scientific Journal
published monthly by the
World Academy of Materials
and Manufacturing Engineering

Quantitative analysis of the fibre content distribution in CFRP composites using thermal non-destructive testing

G. Wróbel [a], Z.M. Rdzawski [a,b], G. Muzia [b], S. Pawlak [a,*]

[a] Institute of Engineering Materials and Biomaterials, Silesian University of Technology, ul. Konarskiego 18a, 44-100 Gliwice, Poland

[b] Institute of Non-Ferrous Metals, ul. Sowińskiego 5, 44-101 Gliwice, Poland

* Corresponding author: E-mail address: sebastian.pawlak@polsl.pl

Received 29.11.2009; published in revised form 01.01.2010

ABSTRACT

Purpose: The primary purpose of present study was to determine the fibre content distribution in CFRP composites using thermal non-destructive testing.

Design/methodology/approach: The experiments have been performed using transient thermography to obtain the thermograms for CFRP and neat resin specimens. From recorded thermograms, the thermal diffusivity values were determined for all materials under investigation and for two different preheating conditions to verify the effect of preheating conditions on obtained results.

Findings: It was found from obtained results that composites with different carbon fibre content had different values of thermal diffusivity. Relationship showed that the thermal diffusivity was a linear function of fibre content in considered materials. It was also found from investigated neat resin specimens that the thermal diffusivity measurement was affected by specimen thickness.

Research limitations/implications: Developed relationships between thermal diffusivity and carbon fibre content is not generalized for all types of CFRP composites (manufactured using a different technology or of different thickness), such specific relationships should be determined for any other composite.

Practical implications: The results obtained from present experiment would be of great importance in the industrial or laboratory applications to evaluate the fibre content distribution in carbon/epoxy composites.

Originality/value: Originality of the present paper is about applying the thermal non-destructive testing to determine the fibre content distribution in CFRP composites.

Keywords: Non-destructive testing; Thermography; Fibre content; CFRP composites

Reference to this paper should be given in the following way:

G. Wróbel, Z.M. Rdzawski, G. Muzia, S. Pawlak, Quantitative analysis of the fibre content distribution in CFRP composites using thermal non-destructive testing, Archives of Materials Science and Engineering 41/1 (2010) 28-36.

PROPERTIES

1. Introduction

Carbon fibre reinforced plastic (CFRP) composites are one of the most attractive materials for high performance applications in modern aerospace and aircraft industry due to their high strength- and stiffness-to-weight ratios and many other advantages [1-3]. It is also known that the mechanical and other properties of fibre reinforced composites are highly fibre content dependent. The effect of fibre content on selected characteristics of composites can be found in the literature [4, 5]. Local reinforcement variations arising from production process decide about out-of-control variations of properties in a given component, which is of great importance for the products with high failure-free requirements. To improve a quality inspection of final product it is necessary to develop a reliable non-destructive testing (NDT) method being able to evaluate the fibre content distribution in CFRP composites.

In a wide range of different NDT techniques, infrared (IR) thermography has been considered so far as an emerging technology [6] and nowadays it is widely used in characterisation of composite materials [7] and is able to detect defects and anomalies in many engineering materials [8]. In the case of polymer composite materials, it is applicable to e.g. detection of cracks, impact damages and fatigue degradation [9].

So far, apart from previous authors' results [10-12], no information has been available on application of NDT thermography for the fibre content evaluation in polymer composite materials. The present paper is a continuation of authors' research program directed towards development of thermal non-destructive testing technique in the field of fibre content evaluation in CFRP composites.

2. Experimental

2.1. Methodology

In order to evaluate the fibre content in considered composites, the method initially proposed by Parker et al. [13], for the thermal diffusivity measurements of homogeneous solids, was applied to determine thermal diffusivity values of non-homogeneous carbon/epoxy specimens.

The method consists in preheating the front surface of specimen using short uniform heat pulse Q and measuring the temperature response on the rear surface. If the heat losses are neglected, the temperature of rear surface is given by [13, 14]:

$$U(L,t) = 1 + 2\sum_{n=1}^{\infty}(-1)^n \exp(-n^2\omega) \tag{1}$$

where:

$$\omega = \pi^2 \alpha t / L^2 \tag{2}$$

and U (L, t) are dimensionless parameters, n is an integer, L – specimen thickness, and

$$U(L, t) = \Delta T(L, t)/\Delta T_M \tag{3}$$

where: ΔT (L, t) is the temperature above ambient at the time t and ΔT_M is the maximum temperature rise.

Parker [13] suggested determining the thermal diffusivity α from normalized temperature – time plot at half the maximum temperature rise (U = 0.5) and then ω = 1.37, and the thermal diffusivity for U = 0.5 can be calculated using equation [13, 14]

$$\alpha = 1.38L^2/\pi^2 t_{0.5}, \tag{4}$$

where, $t_{0.5}$ is the time taken to reach a half maximum temperature.

The standard test method [15] also suggests taking the other point from normalized temperature history plots into consideration (e.g. U = 0.3) and then ω = 0.99, and the thermal diffusivity for U = 0.3 can be calculated using the equation [15]

$$\alpha = 0.99L^2/\pi^2 t_{0.3}. \tag{5}$$

All specimens were investigated using transient thermography to obtain the temperature – time plots from which the thermal diffusivity values for times $t_{0.5}$ and $t_{0.3}$ were determined. To assess the effect of specimen thickness on thermal diffusivity measurement, a group of neat resin specimens was investigated using the same procedure as for CFRP composites.

2.2. Materials

Composite materials were made of plain woven carbon fabric ("Sigratex", "SGL Carbon Group", Germany) and epoxy resin („Epidian 53", "Organika-Sarzyna", Poland). Selected details about constituent materials are shown in Table 1.

Table 1.
The properties of constituent materials

Parameter	Carbon fibre (* fabric)	Epoxy resin
Density	1.70 [g/cm^3]	1.13 [g/cm^3]
Areal weight	240 [g/m^2]*	-
Thermal conductivity coef.	~15.0 [W/mK]	~0.22 [W/mK]

Two main groups of specimens of a square shape (100 by 100 mm) were prepared, including eight CFRP composites with thickness of about 3 and 6 mm and four neat resin specimens with thickness range from 3 to 6 mm. The chosen properties of prepared specimens are shown in Table 2.

Composites were fabricated by hand lay-up with variation of carbon content, using different number of carbon layers with the same total thickness of the specimens.

All specimens before thermographic investigations were painted with a thin matt black coating with an emissivity value of

about 0.95 in order to eliminate reflections, effect of overhead lights or humans and to ensure homogeneity in the specimen surface emissivity.

Table 2.
Properties of specimens tested

No.	Specimen symbol*	Layers amount	Fibre content [%vol.]	Thickness [mm]
CFRP specimens				
1	C302	2	8.4	3.25
2	C304	4	17.0	3.21
3	C305	5	20.6	3.31
4	C306	6	26.4	3.12
5	C604	4	8.6	6.40
6	C606	6	13.4	6.21
7	C610	10	22.2	6.22
8	C612	12	28.1	6.01
Neat resin specimens				
9	300	0	0	3.31
10	400	0	0	4.39
11	500	0	0	4.94
12	600	0	0	6.29

* First number in specimens' symbols indicates the approximate thickness in millimetres, second with third number - amount of fabric layers. Letter "C" is for CFRP composite.

2.3. Apparatus

The apparatus was designed and constructed to provide uniform preheating conditions, such as stable specimen mounting, constant distance between preheating source and specimen and also precise preheating time for all measurements. The scheme of experimental arrangement with devices used is shown in Fig. 1.

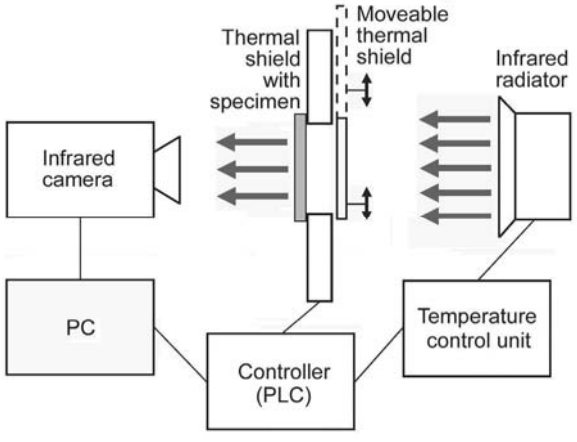

Fig. 1. Scheme of the experimental arrangement

As a thermal wave source a 1200 W black-ceramic infrared radiator with wavelength range of 2-10 μm and surface dimensions of 250 x 62 mm was used.

The temperature variations was measured at the rate of 7.5 images per second and recorded using IR camera ("ThermaCAM^{TM}SC640", "Flir Systems", Sweden) with focal plane array (FPA) detector. For thermograms' analysis the "Researcher Professional 2.9" ("Flir Systems") software was used.

2.4. Procedure of measurements

Each specimen was mounted vertically (parallel to the infrared radiator) in a hole of the thermal shield of the presented apparatus and preheated when moveable thermal shield was opened. The temperature response was recorded by IR-camera from two areas (area 1 and area 2, see Figs. 12-15) of rear surface of specimen tested to compare the conformity of obtained results.

Due to the relatively low conductivity of considered CFRP composites, in comparison with metals, a long-pulse approach was selected to ensure a linear temperature response on rear surface. The preheating time and distance between thermal wave source and specimen (Tab. 3.) was determined experimentally when linear temperature increase on rear surface was observed. During optimisation of preheating conditions, the preheating time for all ~3 mm thick specimens was reduced to 1.0 second due to the too high temperature increase, possibly affecting the thermal properties of the specimen. All developed preheating conditions with investigated specimens are shown in Table 3. Each group of specimens was tested using two different preheating conditions.

Table 3.
Pulse preheating conditions with investigated specimens

Condition	Specimen to radiator distance [mm]	Preheating time [sec]	Investigated specimens
A	20.0	1.0	300, C302, C304, C305, C306
B	30.0	1.0	
C	20.0	2.0	400, 500, 600, C604, C606, C610, C612
D	30.0	2.0	400, 500
E	30.0	3.0	600, C604, C606, C610, C612

3. Results and discussion

3.1. Neat resin specimens

The obtained plots of recorded temperature variations against time for neat resin specimens are shown in Figs. 2-5. The plots clearly show the differences of maximal temperature increase corresponding to different preheating conditions applied for each specimen. It is evident that the longer the preheating time, the higher temperature increase is.

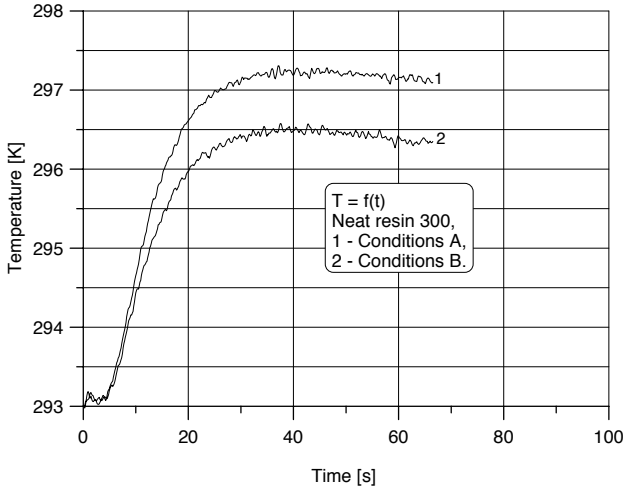

Fig. 2. Temperature variations against time for neat resin 300 specimen (conditions A and B)

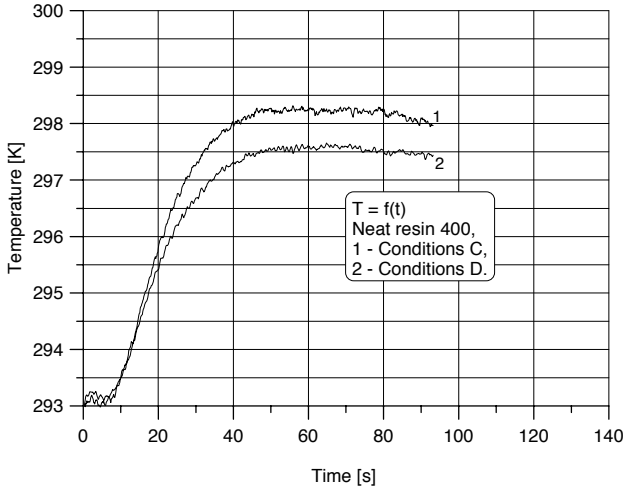

Fig. 3. Temperature variations against time for neat resin 400 specimen (conditions C and D)

It is also evident that the lower the distance between specimen and radiator, the higher temperature increase is.

From all presented temperature – time plots, the thermal diffusivity values were determined according to procedure described in reference [13] and standard test method [15].

Figures 6 and 7 show differences about thermal diffusivity, corresponding to different thickness of neat resin specimens. In general, the thermal diffusivity value increases with specimen thickness increase. This situation shows how high the thermal diffusivity measurement is affected by specimen thickness. The obtained results of thermal diffusivity for $t_{0.5}$ (Fig. 6) varied from $1.30 \cdot 10^{-7}$ to $1.45 \cdot 10^{-7}$ [m^2/s] for 3.31 and 6.29 mm thick specimen, respectively. For $t_{0.3}$ (Fig. 7) the values are lower than for $t_{0.5}$ (Fig. 6), and differences between the two are equal to about $0.05 \cdot 10^{-7}$ [m^2/s].

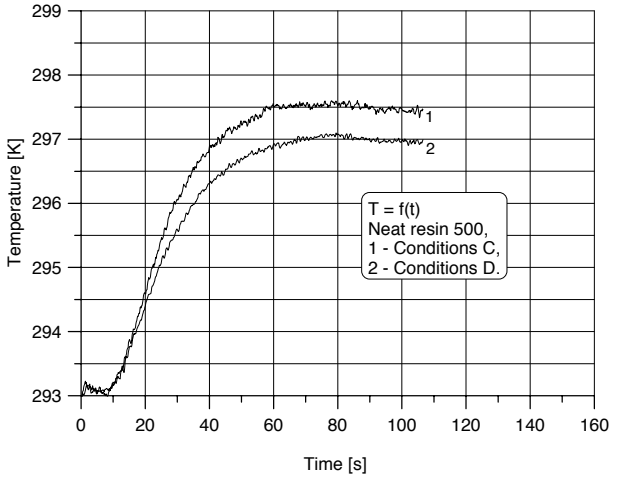

Fig. 4. Temperature variations against time for neat resin 500 specimen (conditions C and D)

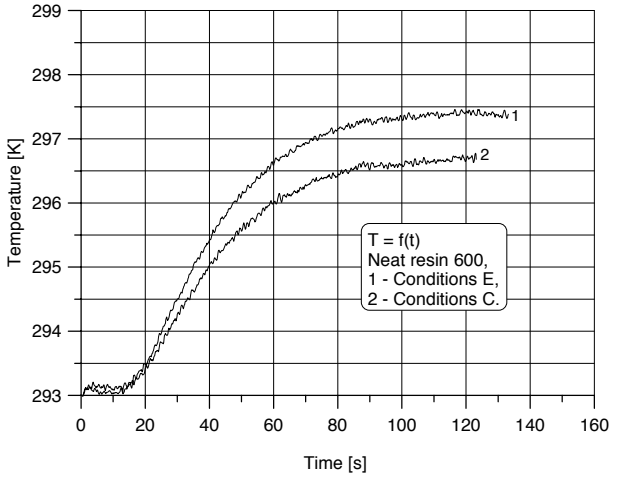

Fig. 5. Temperature variations against time for neat resin 600 specimen (conditions E and C)

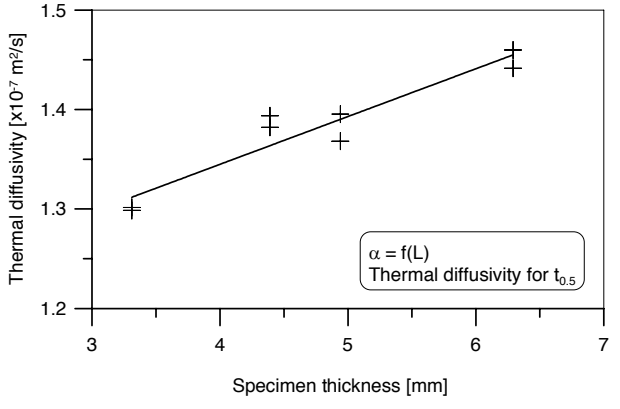

Fig. 6. Thermal diffusivity as a function of specimen thickness for neat resin specimens, calculated for $t_{0.5}$

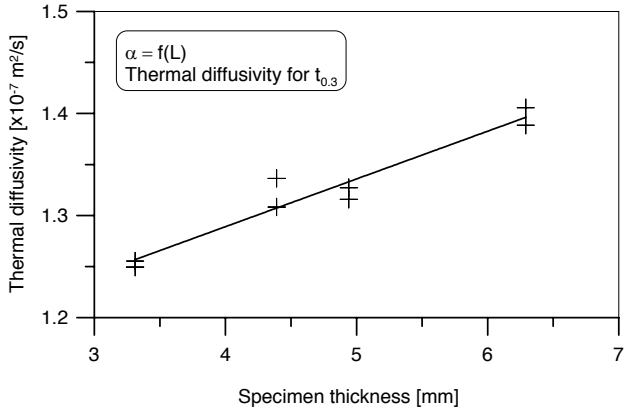

Fig. 7. Thermal diffusivity as a function of specimen thickness for neat resin specimens, calculated for $t_{0.3}$

3.2. CFRP composite specimens

The obtained plots of temperature variations with time for CFRP composites are shown in Figs. 8-11. The vertical axes with temperature were prepared to have the same range from 293 to 298 K (for 3 mm thick specimens) and from 293 to 299 K (for 6 mm thick specimens) for both preheating conditions, to show clearly the differences between temperature increase in both cases.

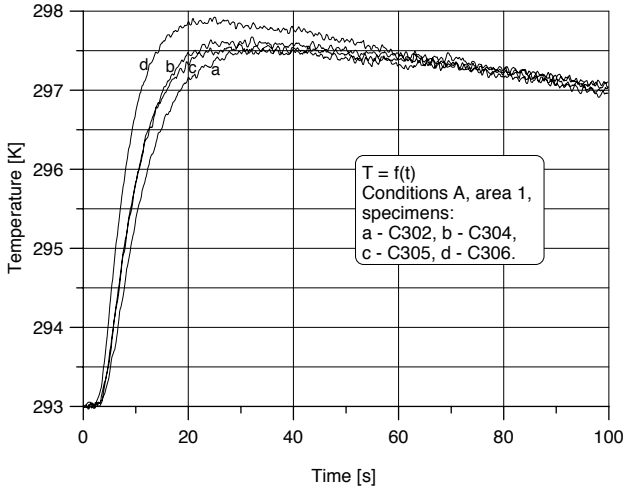

Fig. 8. Temperature variations against time for: a) C302, b) C304, c) C305, d) C306 specimens (conditions A)

For example, the temperature increase for C306 specimen is equal to about 4.9 K (conditions A) in comparison with about 4.2 K for the same specimen but in the case of conditions B (see Figs. 8 and 9). In both cases the linear temperature response is clearly seen. The transposed sequence of temperature variation plots (a, c, b, d, for 3 mm thick specimens, Figs. 8 and 9) for specimens with an increasing fibre content is due to the effect of differences in thickness of the specimens (see Tab. 2).

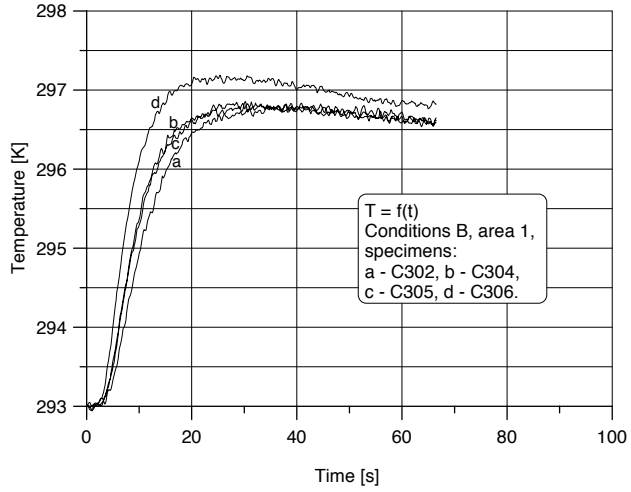

Fig. 9. Temperature variations with time for: a) C302, b) C304, c) C305, d) C306 specimens (conditions B)

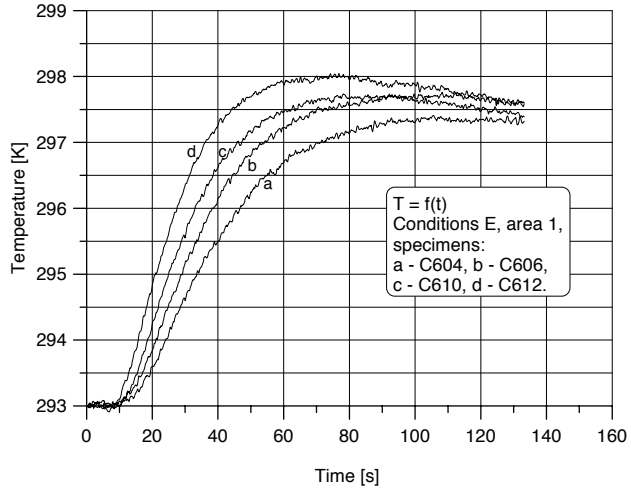

Fig. 10. Temperature variations with time for: a) C604, b) C606, c) C610, d) C612 specimens (conditions E)

For the case of C612, the temperature increase is equal to about 5.1 K (Fig. 10) in comparison with about 4.3 K (Fig. 10) for conditions E and C, respectively.

It can be also observed, that the higher carbon fibre content is, the higher maximal temperature increase is, but direct comparison can be performed only in the case of specimens with near-thickness.

For two specimens with near-thickness (C302 and C304), the thermal images (Figs. 12 and 13) were prepared to present obtained differences in temperature represented by different colour distributions on specimen surface. The same comparison was also performed for 6 mm specimens with near-thickness (C606 and C610). Figures 14 and 15 show the differences with colour distributions on specimen surface for C606 and C610 specimens.

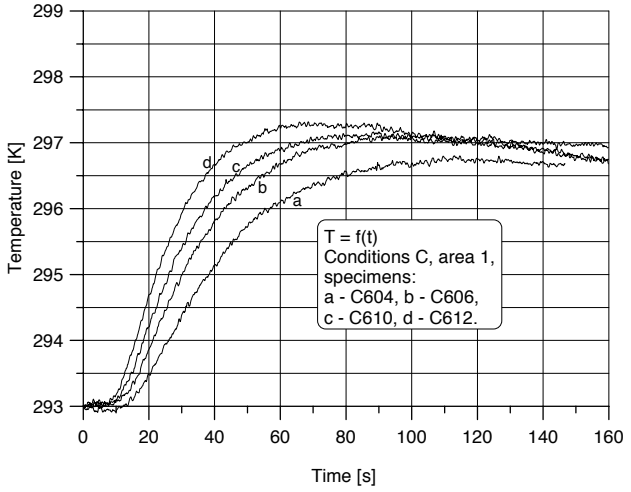

Fig. 11. Temperature variations against time for: a) C604, b) C606, c) C610, d) C612 specimens (conditions C)

The presented thermal images consist of a view of the preheated specimen (centre of the image) and the neighbourhood. At the time of 0 seconds to about 3 seconds (for 3 mm specimens) the specimen as well as the neighbourhood were represented by the same colour on thermal images due to the same temperature and the same mat black coating. The images were prepared as a comparison of two cut images connected together, showing temperature differences.

The thermal images were captured at the time of 10.0 and 20.0 seconds (for 3 mm thick specimen, Figs. 12 and 13) and 20.0 and 33.3 seconds (for 6 mm thick specimen, Figs. 14 and 15) counting from the beginning of the preheating process.

These images were chosen to be representative from all captured images due to the near-thickness of the specimens (C302 and C304, C606 and C610).

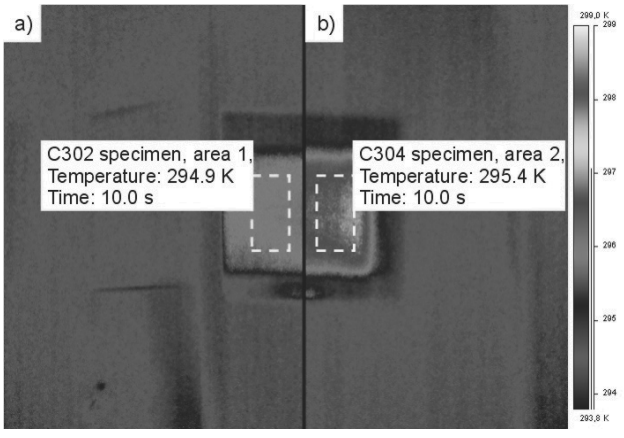

Fig. 12. Comparison of the thermal images of C302 (a) and C304 (b) specimens captured at the rear surfaces (area 1 and 2) after 10.0 seconds

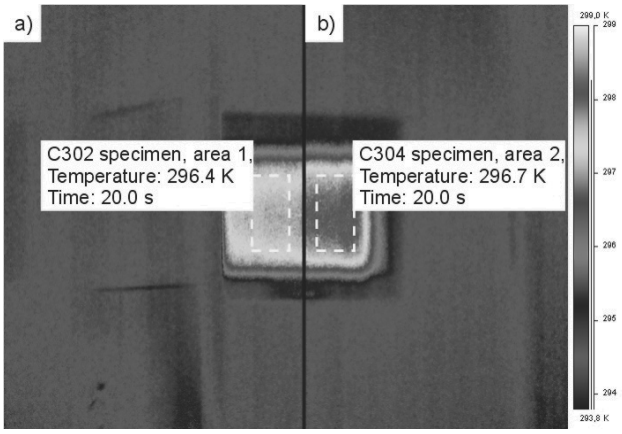

Fig. 13. Comparison of the thermal images of C302 (a) and C304 (b) specimens captured at the rear surfaces (area 1 and 2) after 20.0 seconds

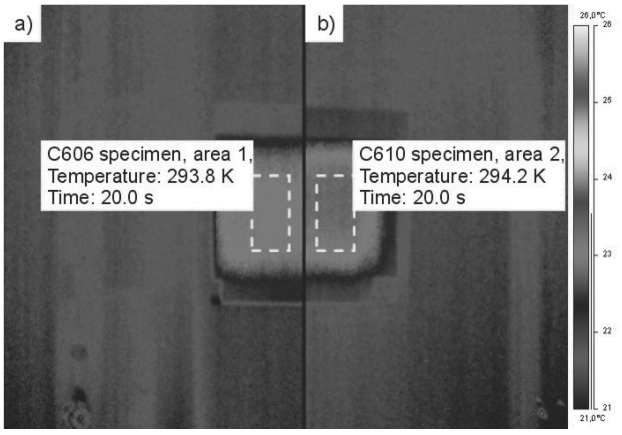

Fig. 14. Comparison of the thermal images of C606 (a) and C610 (b) specimens captured at the rear surfaces (area 1 and 2) after 20.0 seconds

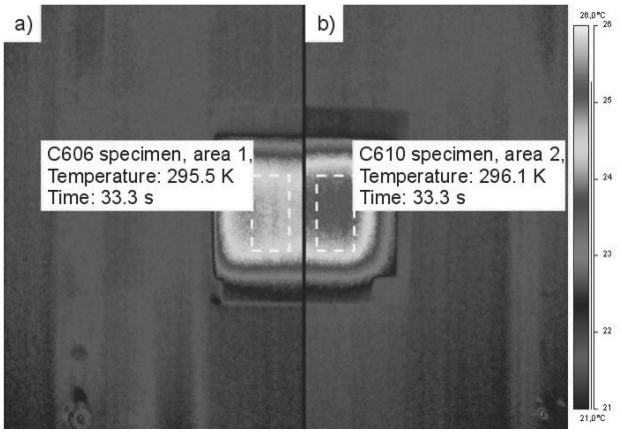

Fig. 15. Comparison of the thermal images of C606 (a) and C610 (b) specimens captured at the rear surfaces (area 1 and 2) after 33.3 seconds

It was clearly seen from thermal images captured at the same time that for each specimen, the higher the carbon content is, the higher the temperature is (area 1 and area 2). Other differences such as temperature growth rate can be only observed on "temperature variations against time" plots (Figs. 8-11) obtained while the temperature recording for all investigated specimens.

From all presented temperature – time plots, the thermal diffusivity values were determined according to procedure described in reference [13] and standard test method [15].

The $t_{0.5}$ and $t_{0.3}$ values taken from normalized temperature plots together with specimen thickness (L) were used to calculate the thermal diffusivity values according to Eqs. 4 and 5, presented above. Obtained graphs (shown in Figs. 16-19) point out that the higher the carbon content is, the higher the thermal diffusivity value is. Despite of different preheating conditions the values for given specimen are similar, which is represented by little scattering of results in Figs. 16-19. These results have been further processed using standard regression technique to obtain the best fitting lines, which equations are presented in legends (Figs. 16-19).

There are insignificant (less than 4%) differences between thermal diffusivity values for $t_{0.5}$ and $t_{0.3}$, indicating that effects of thermal losses caused by long preheating pulse time, radiant energy penetration or relatively high temperature increase on the rear surface can be neglected.

Comparing the straight line equations from Figs. 16 and 18 or Figs. 17 and 19, it can be seen that the thermal diffusivity measurement was affected by specimen thickness, which was discussed above during neat resin specimen's investigation. On the other hand, it is unnecessary to evaluate the actual values of thermal diffusivity for given material in order to develop equations that relate carbon fibre content with thermal diffusivity determined by transient method.

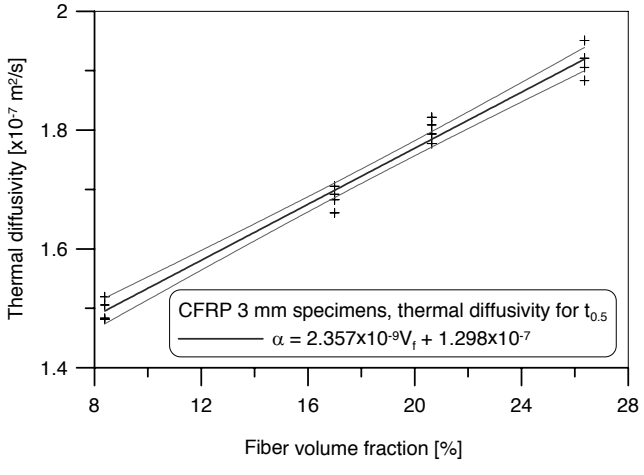

Fig. 16. Thermal diffusivity as a function of fibre content for: C302, C304, C305, C306 specimens, calculated for $t_{0.5}$

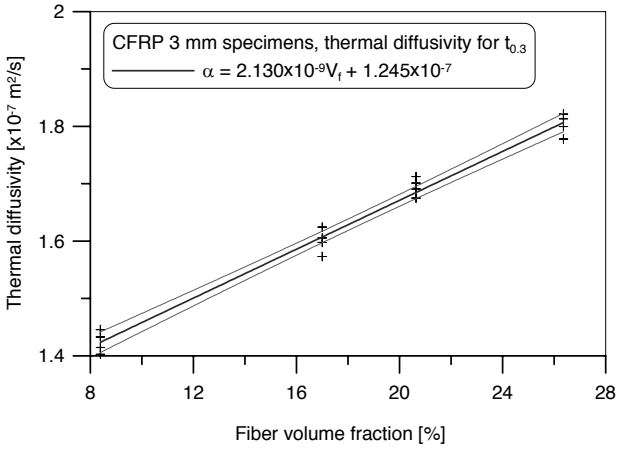

Fig. 17. Thermal diffusivity as a function of fibre content for: C302, C304, C305, C306 specimens, calculated for $t_{0.3}$

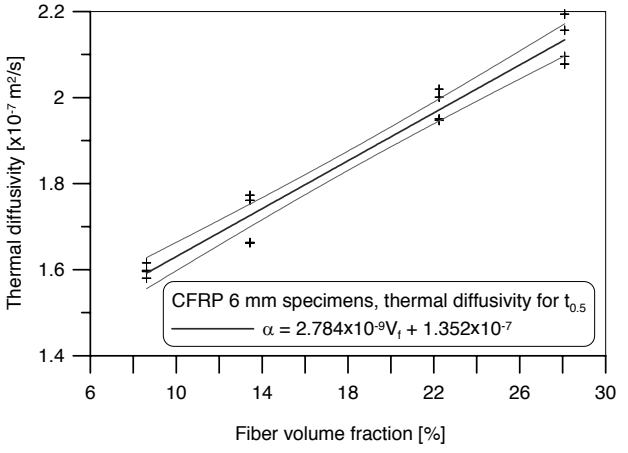

Fig. 18. Thermal diffusivity as a function of fibre content for: C604, C606, C610, C612 specimens, calculated for $t_{0.5}$

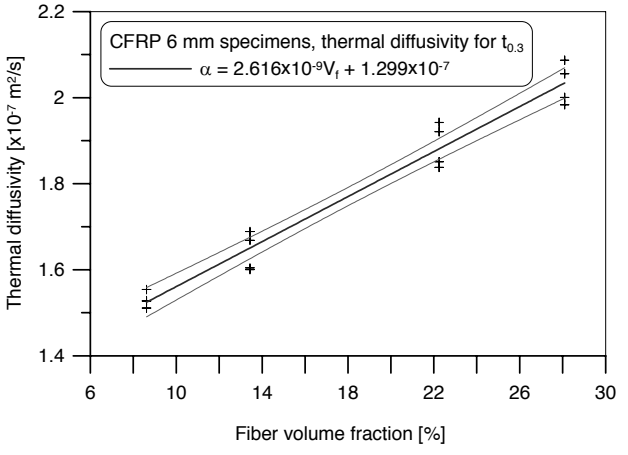

Fig. 19. Thermal diffusivity as a function of fibre content for: C604, C606, C610, C612 specimens, calculated for $t_{0.3}$

The straight line equations presented in the legends in Figs. 16 and 18 were then converted to obtain fibre content V_f. The determination of fibre content V_f can be performed by putting as a value of α the experimentally evaluated thermal diffusivity using transient method.

For example, rewritten straight line equation from legend in Fig. 16,

$$\alpha = 2.357 \cdot 10^{-9} V_f + 1.298 \cdot 10^{-7}, \quad (6)$$

can be directly converted to obtain V_f, so

$$V_f = 42.4 \cdot 10^{7} \alpha - 55.1, \quad (7)$$

where, V_f is expressed in volume percent (%vol.).

The empirical relationship (Eq. 7) gives a quantitative assessment of fibre content in 3 mm thick CFRP specimens.

The same procedure has been also performed for 6 mm thick specimens and after conversion of straight line equation (from legend in Fig. 18), the second empirical relationship is given by

$$V_f = 35.9 \cdot 10^{7} \alpha - 48.5. \quad (8)$$

Taking into account the confidence level (95%), the accuracy of fibre content determination is equal to about ±1.5% (Eq. 7) and about ±2.0% (Eq. 8) for 3 and 6 mm thick specimens, respectively. That indicates the possibility of practical application of transient thermography for the non-destructive testing of fibre content distribution in CFRP composite materials.

4. Conclusions

In the present study, the thermal non-destructive testing was used to assess the carbon fibre content in CFRP composite materials.

The method initially proposed by Parker et al. [13] as a "flash method" for the thermal diffusivity measurements of homogeneous solids was successfully applied to determine the thermal diffusivity values of non-homogeneous CFRP composites. It was also found from investigation results for neat resin specimens that the thermal diffusivity measurement was affected by specimen thickness.

Presented relationship showed that the thermal diffusivity was a linear function of carbon content in considered materials. The developed empirical formulas can be useful to determine the fibre content distribution in many industrial applications.

Acknowledgements

The authors are very grateful to Professor Andrzej Pusz (Department of Metals and Polymers Processing, Gliwice, Poland) for discussions about the theory of heat transfer.

References

[1] L.A. Dobrzański, A. Pusz, A.J. Nowak, Aramid-silicon laminated material with special properties – new perspective of its usage, Journal of Achievements in Materials and Manufacturing Engineering 28/11 (2008) 7-14.

[2] W. Hufenbach, L.A. Dobrzański, M. Gude, J. Konieczny, A. Czulak, Optimization of the rivet joints of the CFRP composite material and aluminium alloy, Journal of Achievements in Materials and Manufacturing Engineering 20 (2007) 119-122.

[3] K. Jamroziak, M. Bocian, Identification of composite materials at high speed deformation with the use of degenerated model, Journal of Achievements in Materials and Manufacturing Engineering 28/1 (2008) 171-174.

[4] O.I. Okoli, G.F. Smith, Failure modes of fibre reinforced composites: The effect o strain rate and fibre content, Journal of Materials Science 33 (1998) 5415-5422.

[5] S.B. Heru, J. Komotori, M. Shimizu, Y. Miyano, Effects of the fibre content on the longitudinal tensile fracture behaviour of uni-directional carbon/epoxy composites, Journal of Materials Processing Technology 67 (1997) 89-93.

[6] D. Bates, G. Smith, D. Lu, J. Hewitt, Rapid thermal non-destructive testing of aircraft components, Composites: Part B 31 (2000) 175-185.

[7] M. Krishnapillai, R. Jones, I.H. Marshall, M. Bannister, N. Rajic, Thermography as a tool for damage assessment, Composite Structures 67 (2005) 149-155.

[8] J. Kaczmarczyk, M. Rojek, G. Wróbel, J. Stabik, A model of heat transfer taking place in thermographic test stand, Journal of Achievements in Materials and Manufacturing Engineering 27/1 (2008) 7-14.

[9] G. Muzia, Z.M. Rdzawski, M. Rojek, J. Stabik, G. Wróbel, Thermographic diagnosis of fatigue degradation of epoxy-glass composites, Journal of Achievements in Materials and Manufacturing Engineering 24/2 (2007) 123-126.

[10] G. Wróbel, G. Muzia, S. Pawlak, Active IR-thermography as a method of fibre content evaluation in carbon/epoxy composites, Archives of Materials Science and Engineering 30/2 (2008) 101-104.

[11] G. Wróbel, Z. Rdzawski, G. Muzia, S. Pawlak, The application of transient thermography for the thermal characterisation of carbon fibre/epoxy composites, Journal of Achievements in Materials and Manufacturing Engineering 36/1 (2009) 49-56.

[12] G. Wróbel, Z. Rdzawski, G. Muzia, S. Pawlak, Determination of thermal diffusivity of carbon/epoxy composites with different fibre content using transient thermography, Journal of Achievements in Materials and Manufacturing Engineering 37/2 (2009) 518-525.

[13] W.J. Parker, R.J. Jenkins, C.P. Butter, G.L. Abbot, Flash method of determining thermal diffusivity, heat capacity

and thermal conductivity, Journal of Applied Physics 32 (1961) 1679-1684.
[14] W.N. dos Santos, P. Mummery, A. Wallwork, Thermal diffusivity of polymers by the laser flash technique, Polymer Testing 24 (2005) 628-634.
[15] PN-EN 821-2:2002, Advanced technical ceramics – Monolithic ceramics – Thermo-physical properties – Part 2: Determination of thermal diffusivity by the laser flash (or heat pulse) method.